Explaining the Effects of T−O−T Bond Angles on NMR Chemical Shifts in Aluminosilicates: A Natural Bonding Orbital (NBO) and Natural Chemical Shielding (NCS) Analysis

Yun Liu,† Hanna Nekvasil,‡ and John Tossell*,†

Department of Chemistry and Biochemistry, University of Maryland, College Park, Maryland 20742, and Geosciences Department, State University of New York at Stony Brook, New York 11794-2100

Received: August 28, 2004; In Final Form: February 3, 2005

It has long been recognized that the ^{29}Si and ^{27}Al NMR chemical shifts for aluminosilicate crystals and glasses correlate to some extent with the T−O−T bond angle (where T is the tetrahedral atom Si or Al). With increasing T−O−T bond angle, the ^{29}Si and ^{27}Al NMR shieldings increase and the shifts thus become more negative. This result has been demonstrated both experimentally and through quantum computations. However, no simple qualitative explanation has ever been given for what appears to be a simple qualitative trend. We here provide such an explanation based upon quantum calculations. We have used high level ab initio NMR shielding calculations, natural bonding orbital (NBO) analysis, and natural chemical shielding (NCS) analysis, performed on model clusters with different T−O−T angles, to obtain an explanation for this trend from an electronic structure point of view. On the basis of both NBO populations and the NCS analysis, the following factors account for the correlation of shift with T−O−T angle: (1) a slight increase in population of the Al−O and Si−O bond orbital electrons and a dramatic change in bond orbital shapes and hybridization (with more s character and less bond bending as the T−O−T angle increases), (2) a movement of one of the lone pairs on O toward the vicinity of the Si or Al as the T−O−T angle increases, and (3) a change in the shielding contribution from the core 2p electrons of Al or Si. The changes in the ^{17}O NMR shift with T−O−T angle are more complex, and the shifts are also more strongly influenced by distant atoms, but some systematic changes in O lone pair contributions can be identified.

I. Introduction

It is a well-known fact that the T−O−T bond angle (here, T is the tetrahedral atom Si or Al) in aluminosilicates can affect the NMR chemical shifts of the T atoms. The effect of the T−O−T angle on NMR shifts has been demonstrated both experimentally and theoretically, by a number of researchers.[1−12] Understanding the nature of the relationship between the chemical shift and the distribution of T−O−T bond angles could potentially lead to important structural information both for crystalline materials with complicated chemical environments and for glasses by providing insights into properties such as the Si/Al ratio, Si/Al ordering, and possible Al−O−Al linkages.[9−11] However, the electronic structure details of the chemical shift/bridging bond angle relationship have remained elusive.

A fundamental difficulty encountered in the interpretation of observed ^{27}Al or ^{29}Si chemical shift/bond angle correlation is the fact that the measured chemical shift reflects the composite effect of four T−O−T bond angles in aluminosilicate materials.[12] However, our previous ab initio calculations on the ^{27}Al NMR properties of Al in tetrahedral coordination have indicated that there is little difference between the calculated isotropic chemical shift if an average T−O−T angle is used or if individual T−O−T bond angles are used provided that the average of each is the same.[13] It appears simply that enlarging one T−O−T angle and reducing another to the same extent in aluminosilicates will increase and decrease the shielding seen by T such that the net effect is no different than if a per tetrahedron average T−O−T angle were used. Hence, the ^{27}Al and ^{29}Si NMR properties correlate at least with the average T−O−T bond angle.

^{17}O NMR parameters could be expected to provide more direct information on the individual T−O−T bond angles. Many early studies on these ^{17}O NMR properties and T−O−T correlation were from ab initio quantum calculations, such as the work from Tossell and his colleagues.[8,14−15] The ^{17}O chemical shift appears to correlate more strongly with parameters such as C_q (quadrupolar coupling constant) of the bridging O, parameters which can also be easily obtained from experiments.[16] Experimental studies also give more and more evidence for this correlation especially after the ^{17}O MQMAS techniques has been widely used.[17−21] Although some people still raised questions about whether the ^{17}O chemical shift can be directly correlated with the T−O−T bond angle,[22−25] recently, from both ab initio calculations and experiments (such as the work from Grandinetti and his collaborators), this correlation has been confirmed very well.[26−28]

However, the question that remains is *why* are the shielding properties of Al, Si, and O atoms affected by the T−O−T angles? From an electronic structure point of view, the NMR shielding properties are determined by the spatial and energetic distribution of surrounding electrons. A change in T−O−T bond angle must somehow involve the relocation of some portion of the surrounding electrons and changes in their energy eigen-

---

* To whom correspondence should be addressed. E-mail: tossell@chem.umd.edu.

† University of Maryland.

‡ State University of New York at Stony Brook.

10.1021/jp046103b CCC: $30.25

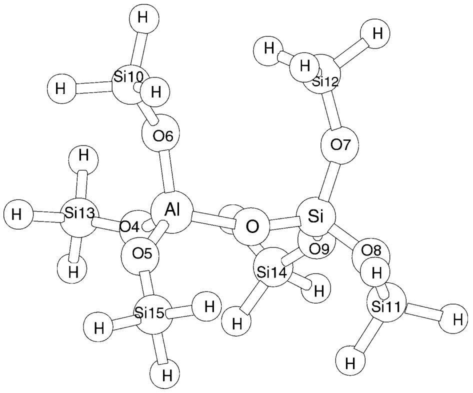

Figure 1. Al−O−Si cluster model.

values, thereby changing the isotropic chemical shift. To investigate this, high level ab initio NMR calculations coupled with both natural bonding orbital (NBO) population analysis and natural chemical shielding (NCS) analysis were performed.[29]

II. Cluster Model

Aluminosilicates such as albite ($NaAlSi_3O_8$) and jadeite ($NaAlSi_2O_6$) as well as some Al-free silicates such as quartz (SiO_2) and their respective glasses consist of an Al and/or Si tetrahedral framework containing rings of various sizes. The best fit to experimental NMR data requires the use of cluster models that mimic these rings as much as possible. However, for the purpose of investigating the NMR trends arising from the variation of a single T−O−T angle, calculations on simple clusters should suffice. Figure 1 shows the simple cluster model $SiAlO(OSiH_3)_6^{-1}$ selected for this work. We also tested a smaller $SiAlO_7H_6^{-}$ cluster, finding essentially the same trends in shieldings and NBO and NCS properties with the T−O−T angle. In this $SiAlO(OSiH_3)_6^{-1}$ cluster model, all of the ∠Al−O−Si and ∠Si−O−Si angles except the central ∠Al−O−Si one are fixed at 144°, simulating the presence of further linkages (or rings) beyond the cluster. Evidence shows that only a very big cluster model containing four- to five-layer atoms can reproduce accurate ∠T−O−T angles during free optimization.[30] We hence use several fixed ∠Al−O−Si and ∠Si−O−Si angles to avoid the interference coming from this direction (the average T−O−T angle of 138° in aluminosilicate glasses was widened to 144° for this study in order to avoid the formation of hydrogen bonds, an artifact arising from the truncation of the cluster by H).[13,31] For this investigation, the central ∠Al−O−Si bond angle was varied from 125 to 175°.

III. Calculation Methods

Geometry Optimization. All geometry calculations were performed using Gaussian98.[32] Potential energy minima were located with the Berny algorithm using redundant internal coordinates.[33] All geometry calculations used the B3LYP (Becke's three-parameter hybrid functional using the LYP correlation functional) method.[34,35] The chosen basis set was the standard polarized split-valence 6-31G*, because the geometry results of 6-31G* often have an accuracy equivalent to that of much larger basis sets.[36]

NMR Calculations. The NMR shielding tensor calculations were performed using the gauge-including atomic orbital (GIAO) method.[37] Although Gaussian98 permits the use of the Hartree−Fock, DFT, and MP2 levels for NMR calculation, the MP2 level proved to be too time-consuming for regular use. Both the HF and DFT methods produced precise *relative* results with the same trend of ∠T−O−T versus the calculated chemical shift for T. The HF/6-311+G(2df,p) level was chosen for the ^{27}Al, ^{29}Si, and ^{17}O NMR calculations discussed below. The methods used have been shown to provide accurate NMR shieldings.[16] We expect that the calculated *changes* in shielding with bridging bond angle will be even more accurate, to fractions of a ppm. In fact, less accurate methods, for example, those using smaller basis sets, typically show the same trends in NMR shifts as a function of angle, and we could employ them in this paper to reduce computational expense. We choose to employ large basis sets to increase the reliability of our results.

Using the GIAO formalism, the isotropic shielding, σ_{iso}, was obtained by averaging the three principal tensor components, σ_{xx}, σ_{yy}, and σ_{zz}. Isotropic chemical shifts, δ_{iso}, were calculated using the relationship $\delta_{iso} = \sigma_{iso}^{ref} - \sigma_{iso}^{molecule}$, where σ_{iso}^{ref} is the chemical shielding value of a reference substance calculated at the same level. For this study, evaluation of the δ_{qs} (quadrupolar shift) for ^{27}Al and ^{17}O was not needed.

Natural Bonding Orbital (NBO) Method.[38−40, 29] The NBO 5.0 program performs the analysis of a many-electron molecular wave function in terms of localized electron pair bonding units. That is, it transforms a given wave function into a localized form corresponding to the one-center ("lone pair") and two-center ("bond") elements of the common Lewis structure picture. We use it for natural population analysis and natural chemical shielding (NCS) analysis. NCS is similar to the old NMR calculation methods such as LORG or IGLO which calculates the shielding as a sum of contributions from each individual localized molecular orbital.[41−44] The NCS analysis can partition the results of the GIAO method into individual magnetic contributions from chemical bonds and lone pairs. [29]

This method has recently been applied to interpret trends in ^{29}Si NMR spectra for heteroatom-substituted sillyllithium compounds.[45]

Both the NBO population and NCS analysis of the cluster in Figure 1 were done for different Al−O−Si bond angles using the same HF/6-311+G(2df,p) level as the NMR calculations. The following factors were considered for the NBO population analysis: (1) *bonding orbitals*, their population and hybrid coefficients; (2) *lone pairs*, their population and hybrid coefficients; (3) *core pair electrons*; and (4) *natural hybrid orbitals (NHO) directionality and "bond bending"*. Since the "Rydberg" orbitals are only weakly occupied, the population variation within them is not easy to assess and was not evaluated here. However, the potential contributions from non-Lewis structures including those of Rydberg orbitals will be discussed in the NCS analysis section below.

IV. Results and Discussion

NMR Results. Table 1 lists the calculated absolute ^{27}Al, ^{29}Si, and ^{17}O NMR shielding values for the cluster in Figure 1 with varying Al−O−Si bond angles. For ease of reference, each oxygen atom has been numbered for the discussion below except the middle one. The middle oxygen will be referred to as "O", and its ^{17}O NMR properties are also shown in Table 1. The magnitudes of shielding changes for ^{27}Al, ^{17}O, and ^{29}Si are ∼7−9 ppm for the 125−175° range.

The shielding of each atom shows the same trend with Si−O−Al bond angle. With increasing Si−O−Al bond angle, shielding increases and chemical shift decreases (i.e., subtracted by references). The quadrupolar coupling constant, C_q, of the middle O also changes with the bond angle over the entire range, 125−175°.

TABLE 1: Variation in Calculated NMR Absolute Shielding Values (ppm) and C_q (MHz) with ∠Si−O−Al Bond Angle

Si−O−Al	125	130	135	140	145	150	155	160	165	170	175
^{27}Al	547.1	547.9	548.6	549.5	550.4	551.2	551.9	552.5	552.9	553.3	553.2
^{29}Si	481.3	482.5	483.7	484.5	485.7	486.8	487.7	488.6	489.3	489.8	490.3
^{17}O	274.8	276.2	277.2	279.0	279.8	280.6	281.4	282.0	282.6	283.0	283.4
C_q of O	3.71	3.88	4.01	4.11	4.23	4.34	4.43	4.51	4.56	4.60	4.63

TABLE 2: Hybridization of O in Al−O and Si−O Bonds with Varying ∠ Al−O−Si

∠Al−O−Si	125°	130°	135°	140°	145°	150°	155°	160°	165°	170°	175°
O(−Al)	sp$^{1.65}$	sp$^{1.50}$	sp$^{1.37}$	sp$^{1.24}$	sp$^{1.12}$	sp$^{1.02}$	sp$^{0.93}$	sp$^{0.86}$	sp$^{0.80}$	sp$^{0.76}$	sp$^{0.74}$
O(−Si)	sp$^{1.78}$	sp$^{1.70}$	sp$^{1.63}$	sp$^{1.59}$	sp$^{1.53}$	sp$^{1.48}$	sp$^{1.45}$	sp$^{1.42}$	sp$^{1.40}$	sp$^{1.38}$	sp$^{1.38}$

TABLE 3: Hybridization of One Lone Pair on O with Varying ∠Al−O−Si

Al−O−Si	125°	130°	135°	140°	145°	150°	155°	160°	165°	170°	175°
% of p	73.3	76.7	79.8	83.2	86.5	89.7	92.7	95.7	98.8	99.93	99.95
hybrid	sp$^{2.77}$	sp$^{3.32}$	sp$^{4.00}$	sp$^{5.01}$	sp$^{6.48}$	sp$^{8.82}$	sp$^{12.8}$	sp$^{22.5}$	sp$^{89.0}$	sp$^{99.99}$	p

NBO Population Analysis Results. *1. Bonding Orbitals. Al−O and Si−O Bonding Orbitals.* With a change in ∠Al−O−Si from 125 to 175°, the Al−O and Si−O bond lengths shorten. However, the T−O bond lengths in aluminosilicates do not correlate with the NMR shielding value for T. In fact, in some cases, slight enlargement of this bond length increases rather than decreases the shielding value of T. As will be shown below, only upon consideration of bond length in combination with other factors (e.g., the location of hybrid orbitals) can the effect of bond length on the shielding value for T be predicted.

The total number of electrons in both Al−O and Si−O bonding orbitals increases slightly with increasing ∠Al−O−Si (i.e., from 1.9679 at 125° to 1.9845 at 175° for Al−O and from 1.9833 to 1.9885 for the Si−O bonding orbital). Concomitant with this increase is a change in the shape of the bonding orbitals. Each bonding orbital is formed by the contribution of an sp^3 hybrid from Al or Si and an sp^x from O. Within the ∠Al−O−Si range 125−175°, the type of hybridization seen for Al and Si remains unchanged, but the type of hybridization for O changes continuously (see Table 2). With more and more s orbital components instead of p orbital components, the bonding orbitals increasingly contract, thereby increasing the electron density between Al (or Si) and O and bringing some electrons closer to Al or Si. This results in more shielding of the Al and Si nuclei.

Al−O4, Al−O5, Al−O6, Si−O7, Si−O8, and Si−O9 Bonding Orbitals. The population of electrons in these bonding orbitals remains unchanged with varying ∠Si−O−Al. The type of hybridization seen for Al (or Si) and O atoms is unchanged in the range 125−175°. From a NBO population point of view, invariance of the electron population and orbital shape implies that these bonding orbitals contribute little to the change in Al (or Si) NMR shielding.

2. Lone Pairs. The configuration of possible electron lone pairs was evaluated for the middle O atom. There are two lone pairs on O; one pair “sticks out” because it contains only a p orbital component, while the other shows sp^x hybridization with both s and p components. With increasing ∠Si−O−Al, one of the lone pairs which with only a p orbital component remains almost unchanged, while the other one with sp^x hybridization changes its shape clearly, exhibiting more and more of a p orbital shape (Table 3). The increased p orbital component implies lower electron density, as the electrons become increasingly diffuse (i.e., removed from the O nucleus). It is possible that a portion of these electrons move closer to Al or Si. If this is the case, then the NMR shielding properties of Al, Si, and O will be affected.

These results also imply why it is difficult to find a simple correlation between the T−O−T bond angle and ^{17}O NMR chemical shift in natural materials. Increased diffuseness of one of the oxygen lone pairs with increasing T−O−T angle could induce some extent of deshielding of O. Although the change in hybridization of both the Si−O and Al−O bonding orbitals should increase the shielding of O (by bringing electrons more closely in line between O and Al or Si), it is difficult to immediately evaluate the net effects on O by this population analysis alone. Furthermore, the Al−O−Si bond angle is only one of the structural factors which can affect the shielding of O. Different cations or different distances to O and the orientation of the nearest lone pairs on other oxygen atoms can also affect the O shielding. NBO population analysis alone cannot yield sufficient information to assess the extent of each effect on the shielding of O. Any simple trend will likely be further obscured in complex natural systems, since with an increasingly diffuse p type orbital component, the lone pair electrons on oxygen can easily interact with the environment close to them.

3. Core Pair Electrons. None of the core pair electrons of Al, Si, or O show changes during the variation of ∠Si−O−Al. Hence, from a population analysis point of view, they do not appear to play a role in changing the ^{27}Al, ^{29}Si, and ^{17}O NMR shielding. However, from later NCS analysis, this is not the case for Al.

4. Natural Hybrid Orbitals (NHO) Directionality and Bond Bending. NBO analysis also yields information about the “direction” of the natural hybrid orbitals, that is, about the direction of components that form the bonding orbitals and lone pairs. Deviations from the line of nuclear centers are used to show the changes of directions of natural hybrid orbitals and thus *bond bending*. For lone pairs, it yields the orientations of the natural hybrid orbitals in terms of polar, θ, and azimuthal, ϕ, angles.

Al−O and Si−O Bond Bending. The extent of bond bending of the Al natural hybrid orbital in Al−O and of the O’s in Si−O changes systematically with increasing T−O−T bond angle (Figure 2), with the natural hybrid orbitals contributed by Al or Si becoming increasingly collinear with the line of nuclear centers. The bending of the O natural hybrid orbital in Al−O bonding changed up to 7.3° at the 145−150° range and then decreased very quickly to 2.0° when the Al−O−Si angle enlarged to 175°. Generally, the extent of bond bending is reduced at large T−O−T angle for all natural hybrid orbitals in Al−O or Si−O bonding.

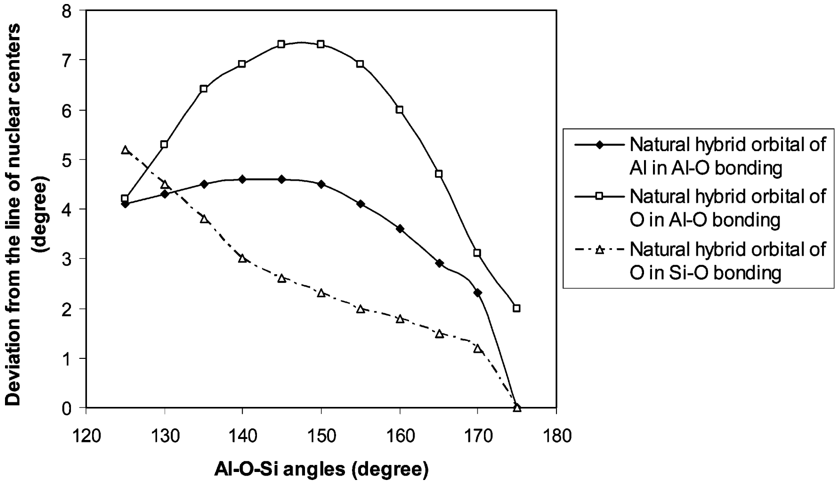

Figure 2. Bending of the natural hybrid orbitals of Al and O in the Al−O bond and O in the Si−O bond.

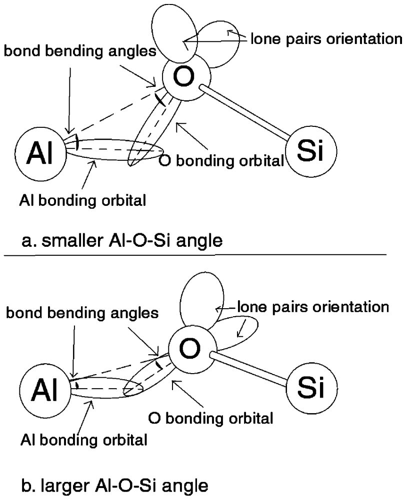

Figure 3. Schematic showing the bond bending angle and lone pair orientation.

Lone Pair Orientations. With increasing T−O−T, lone pairs remain fairly centered between Al and Si but rotate directions. The azimuthal, ϕ, angles of these lone pairs appear to remain around 270° for larger T−O−T bond angles, which is roughly at the midline of the ∠Al−O−Si bond angle for each specific geometry. Looking at the whole picture for the O atom, with increasing ∠T−O−T, one lone pair becomes more diffuse (with more and more p orbital component), and both lone pairs remain balanced between Al and Si (with azimuthal angles remaining at 270°) but with rotated orientations (i.e., different polar angles). Figure 3 shows the rotation orientations of lone pairs with different polar angles.

Summary of NBO Population Analysis. This population analysis suggests that two factors may account for the increase in shielding with increasing T−O−T bond angle: (1) a slight increase in population of the Al−O and Si−O bonding orbital electrons and dramatic change of their electron distribution (with more s orbital component and less bond bending) and orientation (less bending) and (2) increased diffuseness of one of the lone pairs on the O atom and hence its increased removal from the vicinity of O (and perhaps increased proximity to Al or Si).

Natural Chemical Shielding (NCS) Analysis Results. Population analysis cannot directly assess individual contributions to the total shielding in part because empty or weakly occupied orbitals can contribute significantly to the paramagnetic shielding. Hence, NCS analysis is needed and the results can be compared with those of the population analysis method to further the development of a mechanistic model.[29]

NCS results for Al, Si, and O are shown in Tables 4, 5, and 6, respectively. Some NBOs with very tiny contributions have to be ignored for simplicity.

1. Al NCS Analysis. From Table 4, several factors appear to lead to the increases in total shielding with increasing ∠Al−O−Si angle:

(i) The Al−O bonding orbital undergoes an increasing amount of shielding (from −20.5 to −16.9 ppm). This appears to be the dominant cause of the increase in total shielding and was also predicted by NBO population analysis.

(ii) Al−O4, Al−O5, and Al−O6 bonding can also contribute to the shielding increase (from −51.0 to −44.8 ppm).

(iii) The lone pairs on O contribute to the shielding increase but only at larger T−O−T angles.

(iv) Other lone pairs on O4, O5, and O6 contribute a small but stable shielding increase.

These factors all suggest that the total Al NMR shielding should increase with increasing Al−O−Si bond angle. The second and fourth factors are not predicted by a NBO population analysis. NCS analysis also shows that a portion of the core electrons (i.e., 2p orbitals) may see a decrease in shielding, suggesting that these 2p core orbitals can actively take part in small local structure changes, becoming more diffuse, and decrease the Al shielding.

NCS analysis also shows that the so-called “non-Lewis” antibonding or Rydberg orbitals do contribute to the shielding. The results compiled in Table 4 indicate that the total non-Lewis contribution changes from 5.0 to 10.7 ppm with the increase of the ∠Al−O−Si angle. Another interesting observation is that the non-Lewis contribution can even be dominant for some NBO orbitals (i.e., the lone pairs). This justifies the conclusion from population analysis that these lone pairs can become diffuse and may enter empty orbitals. Lone pairs are very sensitive to the surrounding environment and will interact readily with other NBO orbitals.

NCS analysis also shows that the Si−O, O4−Si13, O5−Si15, and O6−Si10 bonding orbitals provide only a small contribution to the shielding increase. This is consistent with the NBO population analysis.

2. Si NCS Analysis. The case for Si is quite different from that for Al (see Table 5). The factors appearing to lead to the Si shielding increase with increasing ∠Al−O−Si angle are the following:

TABLE 4: Results of NCS Analysis of ^{27}Al NMR Shielding Contributions (ppm) from Individual Natural Bonding Orbitals as a Function of ∠Al−O−Si

	∠Al−O−Si										
NBOs	125°	130°	135°	140°	145°	150°	155°	160°	165°	170°	175°
Al−O Lewis	−21.43	−20.94	−20.47	−19.64	−19.36	−19.12	−18.83	−18.38	−17.82	−17.19	−16.97
Al−O non-Lewis	0.89	0.70	0.52	0.33	0.40	0.41	0.42	0.38	0.28	0.11	0.10
subtotal	**−20.54**	**−20.24**	**−19.95**	**−19.31**	**−18.96**	**−18.71**	**−18.41**	**−18.00**	**−17.54**	**−17.08**	**−16.87**
Al−O(4,5,6) Lewis	−48.46	−48.56	−48.87	−48.09	−48.52	−48.01	−47.44	−46.62	−46.01	−45.56	−43.49
Al−O(4,5,6) non-Lewis	−2.58	−2.31	−1.97	−2.03	−1.67	−1.61	−1.50	−1.36	−1.31	−1.24	−1.26
subtotal	**−51.04**	**−50.87**	**−50.84**	**−50.12**	**−50.19**	**−49.62**	**−48.94**	**−47.98**	**−47.32**	**−46.8**	**−44.75**
O−Si Lewis	−1.98	−2.03	−2.08	−2.01	−2.18	−2.28	−2.37	−2.44	−2.48	−2.41	−2.44
O−Si non-Lewis	0.83	0.70	0.57	0.42	0.37	0.33	0.31	0.30	0.29	0.28	0.33
subtotal	**−1.15**	**−1.33**	**−1.51**	**−1.68**	**−1.81**	**−1.95**	**−2.06**	**−2.14**	**−2.19**	**−2.13**	**−2.11**
O4−Si13, O5−Si15, O6−Si10 Lewis	−4.6	−4.65	−4.7	−5.18	−5.00	−5.30	−5.49	−5.64	−5.62	−5.63	−5.44
O4−Si13, O5−Si15, O6−Si10 non-Lewis	1.15	1.08	1.08	1.43	1.39	1.57	1.64	1.68	1.76	1.84	1.01
subtotal	**−3.45**	**−3.57**	**−3.62**	**−3.75**	**−3.61**	**−3.73**	**−3.85**	**−3.96**	**−3.86**	**−3.79**	**−4.43**
Al (core) Lewis	618.56	619.14	619.81	619.23	619.62	619.19	618.31	616.75	615.05	613.5	610.14
Al (core) non-Lewis	−2.7	−2.82	−2.94	−3.00	−2.98	−2.89	−2.73	−2.54	−2.30	−2.17	−2.06
subtotal	**615.86**	**616.32**	**616.87**	**616.23**	**616.64**	**616.3**	**615.58**	**614.21**	**612.75**	**611.33**	**608.08**
O (lone pair 1) Lewis	0.89	0.90	0.89	0.82	0.74	0.70	0.61	0.50	0.48	0.55	0.42
O (lone pair 1) non-Lewis	−0.28	−0.26	−0.22	0.04	0.18	0.45	0.76	1.14	1.52	1.79	1.95
O (lone pair 2) Lewis	0.53	0.56	0.59	0.63	0.65	0.67	0.66	0.63	0.57	0.41	0.35
O (lone pair 2) non-Lewis	0.88	0.71	0.56	0.57	0.52	0.64	0.84	1.14	1.44	1.84	2.04
subtotal	**2.02**	**1.91**	**1.82**	**2.06**	**2.09**	**2.46**	**2.87**	**3.41**	**4.01**	**4.59**	**4.76**
O4, O5, O6 (lone pairs) Lewis	−1.16	−0.93	−0.73	−0.42	−0.22	0.04	0.18	0.14	0.12	0.06	−0.52
O4, O5, O6 (lone pairs) non-Lewis	8.15	8.07	8.03	7.98	7.92	7.88	7.98	8.22	8.38	8.46	10.19
subtotal	**6.99**	**7.14**	**7.30**	**7.56**	**7.70**	**7.92**	**8.16**	**8.36**	**8.50**	**8.52**	**9.67**
Lewis	**542.08**	**543.27**	**544.27**	**545.31**	**545.68**	**545.88**	**545.67**	**545.04**	**544.39**	**543.77**	**542.48**
non-Lewis	**4.99**	**4.59**	**4.36**	**4.20**	**4.71**	**5.32**	**6.25**	**7.47**	**8.54**	**9.48**	**10.71**
total	**547.08**	**547.85**	**548.63**	**549.51**	**550.39**	**551.21**	**551.91**	**552.51**	**552.94**	**553.25**	**553.18**

TABLE 5: Results of NCS Analysis of Si NMR Shielding Contributions (ppm) from Individual Natural Bonding Orbitals as a Function of ∠Al−O−Si

	∠Al−O−Si										
NBOs	125°	130°	135°	140°	145°	150°	155°	160°	165°	170°	175°
Si−O Lewis	−47.92	−46.04	−43.50	−41.00	−39.69	−38.72	−37.88	−37.43	−37.17	−37.18	−36.43
Si−O non-Lewis	6.23	5.80	5.29	4.85	4.70	4.67	4.66	4.66	4.70	4.69	4.58
subtotal	**−41.69**	**−40.24**	**−38.21**	**−36.15**	**−34.99**	**−34.05**	**−33.22**	**−32.77**	**−32.47**	**−32.49**	**−31.85**
Si−O(7,8,9) Lewis	−161.65	−165.10	−168.54	−172.43	−173.89	−174.75	−175.37	−175.83	−175.93	−176.17	−179.09
Si−O(7,8,9) non-Lewis	20.10	20.43	20.61	20.78	21.10	21.34	21.54	21.73	21.79	21.76	22.08
subtotal	**−141.55**	**−144.67**	**−147.93**	**−151.65**	**−152.79**	**−153.41**	**−153.83**	**−154.10**	**−154.14**	**−154.41**	**−157.01**
O−Al Lewis	−8.52	−8.20	−8.09	−7.75	−7.58	−7.43	−7.23	−6.99	−6.85	−6.62	−6.61
O−Al non-Lewis	7.43	6.76	6.21	5.44	4.69	4.02	3.31	2.62	2.10	1.70	1.47
subtotal	**−1.09**	**−1.44**	**−1.88**	**−2.31**	**−2.89**	**−3.41**	**−3.92**	**−4.37**	**−4.75**	**−4.92**	**−5.14**
O7−Si12, O8−Si11, O9−Si14 Lewis	−12.15	−12.15	−13.14	−15.05	−15.8	−16.02	−16.18	−16.22	−16.29	−16.22	−16.00
O7−Si12, O8−Si11, O9−Si14 non-Lewis	12.28	12.81	13.96	14.96	15.84	16.15	16.29	16.28	16.24	16.10	16.43
subtotal	**0.13**	**0.66**	**0.82**	**−0.09**	**0.04**	**0.13**	**0.11**	**0.06**	**−0.05**	**−0.12**	**0.43**
Si (core) Lewis	696.82	700.13	703.52	707.06	708.49	709.50	710.13	710.56	710.79	711.31	714.15
Si (core) non-Lewis	−6.02	−6.12	−6.16	−6.22	−6.31	−6.35	−6.42	−6.48	−6.55	−6.64	−6.92
subtotal	**690.80**	**694.01**	**697.36**	**700.84**	**702.18**	**703.15**	**703.71**	**704.08**	**704.24**	**704.67**	**707.23**
O (lone pair1) Lewis	3.20	2.83	2.40	2.11	1.71	1.37	1.07	0.83	0.70	0.78	0.99
O (lone pair 1) non-Lewis	−7.32	−6.78	−6.23	−6.07	−5.47	−4.86	−4.14	−3.30	−2.41	−2.09	−2.67
O (lone pair 2) Lewis	0.46	0.57	0.72	0.75	0.78	0.80	0.80	0.83	0.80	0.76	0.97
O (lone pair 2) non-Lewis	−0.69	−1.27	−1.99	−2.27	−2.29	−2.36	−2.33	−2.38	−2.57	−2.38	−2.59
subtotal	**−4.35**	**−4.65**	**−5.10**	**−5.48**	**−5.27**	**−5.05**	**−4.60**	**−4.02**	**−3.48**	**−2.93**	**−3.30**
O7, O8, O9 (lone pairs) Lewis	12.75	14.60	17.58	22.17	22.96	23.53	23.87	24.03	24.23	24.37	25.43
O7, O8, O9 (lone pairs) non-Lewis	−29.76	−31.67	−34.84	−38.80	−39.58	−40.19	−40.46	−40.47	−40.48	−40.51	−41.61
subtotal	**−17.01**	**−17.07**	**−17.26**	**−16.63**	**−16.62**	**−16.66**	**−16.59**	**−16.44**	**−16.25**	**−16.14**	**−16.18**
Lewis	**483.15**	**486.88**	**491.42**	**496.76**	**497.82**	**499.18**	**500.13**	**500.76**	**501.27**	**502.07**	**504.75**
non-Lewis	**−1.90**	**−4.39**	**−7.77**	**−12.23**	**−12.14**	**−12.43**	**−12.41**	**−12.18**	**−11.99**	**−12.23**	**−14.47**
total	**481.25**	**482.49**	**483.65**	**484.53**	**485.68**	**486.75**	**487.73**	**488.58**	**489.28**	**489.84**	**490.28**

(i) The 2p core electrons. Their shielding contribution can be increased from 690.8 to 707.2 ppm.

(ii) The Si−O bonding (from −41.7 to −31.9 ppm).

(iii) The lone pairs on O (from −4.4 to −2.9 ppm).

Once again, we see the Si core electrons such as those for Al have an important role in this T−O−T angle versus the NMR story. This is a little surprise for us, and we did not see it from NBO population analysis.

The lone pairs on O7, O8, and O9 also have small contributions on the shielding increase. The Si−O7, Si−O8, and Si−O9 bonding orbitals have a strong negative contribution to the Si shielding.

3. O NCS Analysis. ^{17}O NMR shielding sources are quite complicated (see Table 6). The overall total ^{17}O NMR shielding is only increased a few ppm, but some NBO contributions can be dramatically changed. The most dramatic changes appear attributable to the lone pair of the middle O. Its shielding contribution can decrease as much as 67 ppm. However, when combined with the shielding contribution from Al−O and Si−O bonding orbitals, the net change is small. Hence, the O case is

TABLE 6: O NMR Shielding Contribution from Individual Natural Bonding Orbital by NCS Analysis (in ppm).

	∠Al−O−Si										
NBOs	125°	130°	135°	140°	145°	150°	155°	160°	165°	170°	175°
Al−O Lewis	−80.36	−77.72	−75.28	−66.82	−66.72	−62.14	−58.1	−52.06	−45.01	−36.71	−40.32
Al−O non-Lewis	4.84	4.98	4.92	5.16	4.09	3.45	2.62	1.92	1.72	1.98	1.17
subtotal	**−75.52**	**−72.74**	**−70.36**	**−61.66**	**−62.63**	**−58.69**	**−55.48**	**−50.14**	**−43.29**	**−34.73**	**−39.15**
Si−O Lewis	−123.72	−124.53	−127.56	−129.16	−127.77	−124.86	−120.4	−113.63	−108.63	−99.81	−97.42
Si−O non-Lewis	3.27	2.81	2.11	1.48	0.70	−0.20	−1.14	−1.99	−2.73	−3.40	−3.70
subtotal	**−120.45**	**−121.72**	**−125.45**	**−127.68**	**−127.07**	**−125.06**	**−121.54**	**−115.62**	**−111.36**	**−103.21**	**−101.12**
Si−O(7,8,9) Lewis	−5.31	−5.61	−5.70	−5.63	−5.56	−5.44	−5.22	−5.01	−4.74	−4.52	−4.44
Si−O(7,8,9) non-Lewis	−3.81	−2.94	−1.96	−1.30	−1.08	−0.89	−0.72	−0.56	−0.61	−0.58	−0.42
subtotal	**−9.12**	**−8.55**	**−7.66**	**−6.93**	**−6.64**	**−6.33**	**−5.94**	**−5.57**	**−5.35**	**−5.10**	**−4.86**
Al−O(4,5,6) Lewis	−3.55	−3.71	−3.83	−3.51	−3.69	−3.65	−3.36	−2.77	−2.00	−1.29	−0.23
Al−O(4,5,6) non-Lewis	−3.10	−2.64	−2.22	−1.77	−1.24	−0.70	−0.20	0.23	0.72	0.92	0.77
subtotal	**−6.65**	**−6.35**	**−6.05**	**−5.28**	**−4.93**	**−4.35**	**−3.56**	**−2.54**	**−1.28**	**−0.37**	**0.54**
Al (core) Lewis	−1.88	−1.95	−2.01	−2.04	−2.13	−2.16	−2.13	−2.04	−1.77	−1.52	−1.17
Al (core) non-Lewis	0.17	0.20	0.23	0.26	0.29	0.31	0.33	0.32	0.29	0.26	0.20
Si (core) Lewis	−1.54	−1.53	−1.49	−1.45	−1.5	−1.53	−1.53	−1.49	−1.45	−1.4	−1.34
Si (core) non-Lewis	0.07	0.09	0.10	0.14	0.16	0.19	0.21	0.22	0.23	0.23	0.25
subtotal	**−3.18**	**−3.19**	**−3.17**	**−3.09**	**−3.18**	**−3.19**	**−3.12**	**−2.99**	**−2.70**	**−2.43**	**−2.06**
O (core) Lewis	**276.48**	**276.47**	**276.45**	**276.44**	**276.42**	**276.41**	**276.4**	**276.38**	**276.38**	**276.37**	**276.36**
O (lone pair 1) Lewis	94.63	94.2	95.76	91.59	88.53	84.34	80.19	78.23	85.94	89.14	82.05
O (lone pair 1) non-Lewis	−8.38	−8.68	−8.53	−7.72	−7.60	−7.21	−6.53	−5.32	−3.54	−2.66	−2.07
O (lone pair 2) Lewis	136.31	135.91	134.51	130.89	135.08	132.85	128.31	115.25	91.49	66.43	71.99
O (lone pair 2) non-Lewis	−5.64	−5.51	−5.38	−4.97	−5.13	−5.05	−4.80	−4.36	−4.07	−2.82	−2.03
subtotal	**216.92**	**215.92**	**216.36**	**209.79**	**210.88**	**204.93**	**197.17**	**183.8**	**169.82**	**150.09**	**149.94**
O4−O9 (lone pairs) Lewis	−1.80	−1.69	−1.46	−2.21	−2.40	−2.65	−3.09	−3.65	−4.27	−5.04	−5.64
O4−O9 (lone pairs) non-Lewis	−1.65	−1.45	−0.50	0.08	−0.08	0.01	0.87	2.39	4.65	7.12	9.22
subtotal	**−3.45**	**−3.14**	**−1.96**	**−2.13**	**−2.48**	**−2.64**	**−2.22**	**−1.26**	**0.38**	**2.08**	**3.58**
Lewis	**292.8**	**293.39**	**292.86**	**292.73**	**294.77**	**295.63**	**295.46**	**293.46**	**289.76**	**284.99**	**282.52**
non-Lewis	**−17.99**	**−17.20**	**−15.63**	**−13.76**	**−14.93**	**−15.01**	**−14.11**	**−11.43**	**−7.16**	**−2.03**	**0.87**
Total	**274.82**	**276.20**	**277.23**	**278.97**	**279.84**	**280.63**	**281.35**	**282.03**	**282.59**	**282.96**	**283.40**

rather unusual; with the small and stable overall total O shielding increase, many NBOs have dramatic contributions.

The factors appearing to lead to the O shielding *increase* with increasing ∠Al−O−Si angle are the following:

(i) The Al−O bonding orbital (from −75.5 to −34.7 ppm).

(ii) The Si−O bonding orbital (increasing contributions only occur at larger angles).

(iii) The Al−O(4,5,6) and Si−O(7,8,9) bonding orbitals.

(iv) The lone pairs on all of the nearby O atoms (O4−O9).

Compared to the dramatic changes from Al−O, Si−O, and the lone pairs on the middle O, all of the other contributions that form the above points iii and iv are rather small. The core electrons for Al, Si, and O itself can have even smaller contributions to the O shielding increase. At first, they may belong to those minor factors and could be ignored. However, if you consider the small total O shielding change for the whole Al−O−Si angle range, they should be kept for careful discussion as well. This is why the O case is so tricky because the most dominant factors (such as the lone pair) can be easily affected by the environment (e.g., cations and other long distance disturbances).

Population analysis has showed that with increasing p component of one of the lone pairs on O its shielding contribution decreases. The shortening of Si−O and Al−O bonds will likely give rise to more shielding of O. These two points were fully supported by NCS analysis here: the dramatic shielding decrease from the middle O and the large shielding increase from Al−O and Si−O bonding. However, population analysis cannot determine the nature of the shielding contributions from the lone pairs on O(4−9) or from the Al−O(4,5,6) and Si−O(7,8,9) bonding orbitals. Some of them have more non-Lewis characters. These are the places that need the power of the NCS method.

V. Summary

The combination of NBO population and natural chemical shielding (NCS) analysis provides a model for the observed effect of the T−O−T bond angle on the NMR chemical shifts of T (i.e., Al or Si) in aluminosilicates and aluminosilicate glasses. With increasing T−O−T bond angle, the electron population between T and O increases slightly, but more dramatic changes occur in the shapes of the bonding orbitals. The electrons move closer to both T and O (changing their hybridization from more p-like to more s-like, and the bonding orbital directions become more collinear with the nuclear centers of T and O. The movement of one lone pair on O closer to Al or Si also contributes to the shielding of both Al and Si. NCS results support the idea that these two factors are primary in causing the correlation of NMR chemical shifts with T−O−T bond angle. NCS analysis also shows that other NBOs (i.e., Al−O(4,5,6) and Si−O(7,8,9) bonding and the lone pair on O(4−9)) can have some, albeit minor, contributions. Even the core 2p orbitals can contribute significantly to the shift trends in the case of Si. Similar significant changes in core contributions have been seen in the NCS analysis of silyllithium compounds by Auer et al.[45] Several rather complicated effects have been identified and discussed to explain the correlation between the shielding of O and the T−O−T bond angle.

Acknowledgment. This work was supported by NSF grant EAR-0001031 and DOE grant DE-FG02-94ER14467. Some of the calculations were performed using Gaussian98 on the Carnegie Alpha Cluster, which is supported in part by NSF MRI grant AST-9976645. We thank Dr. Jonathan A. Bohmann for the help on NCS calculations and Dr. Wei Yang (Chem. Department, University of Harvard) for helpful discussion.

References and Notes

(1) Eckert, H. *Prog. Nucl. Magn. Reson. Spectrosc.* **1992**, *24*, 159−293 (part 3).

(2) Smith, J. V.; Blackwell, C. S. *Nature* **1983**, *303*, 223.

(3) Ramdas, S.; Klinowski, J. *Nature* **1984**, *308*, 521.

(4) Engelhardt, G.; Radeglia, R. *Chem. Phys. Lett*. **1984**, *108*, 207.

(5) Mauri, F.; Pasquarello, A.; Pfrommer, B. G.; Yoon, Y. G.; Louie, S. G. *Phys. Rev. B* **2000**, *62*, R4786.

(6) Janes, N.; Oldfield, E. *J. Am. Chem. Soc*. **1985**, *107*, 6769.

(7) Sherriff, B. L.; Grundy, H. D. *Nature* **1988**, *332*, 819.

(8) Tossell, J. A.; Lazzeretti, P. *Phys. Chem. Miner*. **1988**, *15*, 564.

(9) Kirkpatrick, R. J. *Rev. Mineral*. **1988**, *18*, 341.

(10) Lee, S. K.; Stebbins, J. F. *Am. Mineral*. **1999**, *84*, 937.

(11) Tossell, J. A. *Rev. Mineral*. **2001**, *42*, 435.

(12) Farnan, I.; Grandinetti, P. J.; Baltisberger, J. H.; Stebbins, J. F.; Werner, U.; Eastman, M. A.; Pines, A. *Nature* **1992**, *358*, 31.

(13) Liu, Y.; Nekvasil, H. *Am. Mineral*. **2001**, *86*, 491.

(14) Tossell, J. A.; Lazzeretti, P. *Chem. Phys. Lett.* **1987**, *112*, 205.

(15) Lindsay, C. G.; Tossell, J. A. *Phys. Chem. Miner.* **1991**, *18*, 191.

(16) Xue, X.; Kanzaki, M. *Phys. Chem. Miner*. **1998**, *26*, 14.

(17) Maekawa, H.; Florian, P.; Massiot, D.; Kiyono, H.; Nakamura, M. *J. Phys. Chem.* **1996**, *100*, 5525.

(18) Dirken, P. J.; Kohn, S. C.; Smith, M. E.; van Eck, E. R. H. *Chem. Phys. Lett.* **1997**, *266*, 568.

(19) Stebbins, J. F.; Xu, Z. *Nature* **1997**, *390*, 60.

(20) Xu, Z.; Stebbins, J. F. *Solid State Nucl. Magn. Reson.* **1998**, *11*, 243.

(21) Vermillion, K. E.; Florian, P.; Grandinetti, P. J. *J. Chem. Phys.* **1998**, *108*, 7274.

(22) Lee, S. K.; Stebbins, J. F. *J. Phys. Chem. B* **2000**, *104*, 4091.

(23) Lee, S. K. *J. Phys. Chem. B* **2004**, *108*, 5889.

(24) Bull, L. M.; Cheetham, A. K.; Anupold, T.; Reinhold: A.; Samoson, A.; Sauer, J.; Bussemer, B.; Lee, Y.; Gann, S.; Shore, J.; Pines, A.; Dupree, R. *J. Am. Chem. Soc.* **1998**, *120*, 3510.

(25) Bull, L. M.; Bussemer, B.; Anupold, T.; Reinhold, A.; Samoson, A.; Sauer, J.; Cheetham, A. K.; Dupree, R. *J. Am. Chem. Soc.* **2000**, *122*, 4948.

(26) Pingel, U. T.; Amoureux, J. P.; Anupold, T.; Bauer, F.; Ernst, H.; Fernandez, C.; Freude, D.; Samoson, A. *Chem. Phys. Lett.* **1998**, *294*, 345.

(27) Freude, D.; Loeser, T.; Michel, D.; Pingel, U.; Prochnow, D. *Solid State Nucl. Magn. Reson.* **2001**, *20*, 46.

(28) Clark, T. M.; Grandinetti, P. J.; Florian, P.; Stebbins, J. F. *J. Phys. Chem. B* **2001**, *105*, 12257.

(29) Clark, T. M.; Grandinetti, P. J. *J. Phys.: Condens. Matter* **2003**, S2387.

(30) Clark, T. M.; Grandinetti, P. J.; Florian, P.; Stebbins, J. F. *Phys. Rev. B* **2004**, *70*, 064202.

(31) Bohmann, J. A.; Weinhold, F.; Farrar, T. C. *J. Chem. Phys.* **1997**, *107*, 1173.

(32) Bussemer, B.; Schröder, K.; Sauer, J. *Solid State Nucl. Magn. Reson.* **1997**, *9*, 155.

(33) Geisinger, K. L.; Gibbs, G. V.; Navrotsky, A. *Phys. Chem. Miner*. **1985**, *11*, 266.

(34) Frisch, M. J.; Trucks, G. W.; Schlegel, H. B.; Scuseria, G. E.; Robb, M. A.; Cheeseman, J. R.; Zakrzewski, V. G.; Montgomery, J. A.; Stratmann, R. E.; Burant, J. C.; Dapprich, S.; Millam, J. M.; Daniels, A. D.; Kudin, K. N.; Strain, M. C.; Farkas, O.; Tomasi, J.; Barone, V.; Cossi, M.; Cammi, R.; Mennucci, B.; Pomelli, C.; Adamo, C.; Clifford, S.; Ochterski, J.; Petersson, G. A.; Ayala, P. Y.; Cui, Q.; Morokuma, K.; Malick, D. K.; Rabuck, A. D.; Raghavachari, K.; Foresman, J. B.; Cioslowski, J.; Ortiz, J. V.; Stefanov, B. B.; Liu, G.; Liashenko, A.; Piskorz, P.; Komaromi, I.; Gomperts, R.; Martin, R. L.; Fox, D. J.; Keith, T.; Al-Laham, M. A.; Peng, C. Y.; Nanayakkara, A.; Gonzalez, C.; Challacombe, M.; Gill, P. M. W.; Johnson, B.; Chen, W.; Wong, M. W.; Andres, J. L.; Gonzalez, C.; Head-Gordon, M.; Replogle, E. S.; Pople, J. A. *Gaussian98*, revision A.7; Gaussian, Inc.: Pittsburgh, PA, 1998.

(35) Peng, C.; Ayala, P. Y.; Schlegel, H. B.; Frisch, M. J. *J. Comput. Chem*. **1996**, *17*, 49.

(36) Lee, C.; Yang, W.; Parr, R. G. *Phys. Rev. B* **1988**, *37*, 785.

(37) Becke, A. D. *J. Chem. Phys.* **1993**, *98*, 1372.

(38) Foresman, J. B.; Frisch, A. E. *Exploring Chemistry With Electronic Structure Methods*, 2nd ed.; Gaussian, Inc.: Pittsburgh, PA, 1996.

(39) Ditchfield, R. *Mol. Phys.* **1974**, *27*, 789.

(40) Glendening, E. D.; Badenhoop, J. K.; Reed, A. E.; Carpenter, J. E.; Bohmann, J. A.; Weinhold, F. *NBO*, version 5.0; Theoretical Chemistry Institute, University of Wisconsin: Madison, WI, 2000.

(41) Carpenter, J. E.; Weinhold, F. *THEOCHEM* **1988**, *169*, 41.

(42) Reed, A. E.; Curtiss, L. A.; Weinhold, F. *Chem. Rev.* **1988**, *88*, 899.

(43) Schindler, M.; Kutzelnigg, W. *J. Chem. Phys*. **1982**, *76*, 1919.

(44) Kutzelnigg, W. In *Nuclear Magnetic Shieldings and Molecular Structure*; Tossell, J. A., Ed.; NATO ASI Series C, Vol. 386; Kluwer: Boston, MA, 1993.

(45) Hansen, A. E.; Bouman, T. D. *J. Chem. Phys.* **1989**, *76*, 3552.

(46) Hansen, A. E.; Bouman, T. D. In *Nuclear Magnetic Shieldings and Molecular Structure*; Tossell, J. A.; NATO ASI Series C, Vol. 386; Kluwer: Boston, MA, 1993.

(47) Auer, D.; Kaupp, M.; Strohmann, C. *Organometallics* **2004**, *23*, 3647.